Magnetohydrodynamics and Aspect Ratio Effects on Double Diffusive Mixed Convection and Their Prediction: Linear Regression Model

Shivananda Moolya [a,b], Satheesh Anbalagan [*,a], Neelamegam Rajan Devi[c], Rekha Moolya[d]

[a]*School of Mechanical Engineering, Vellore Institute of Technology, Vellore, Tamilnadu, INDIA-632014.*
[b]*University of Technology and Applied Sciences, PO Box 74, Al-Khuwair Postal code 133, Sultanate of Oman.*
[c]*Department of Physics, Auxilium College (Autonomous), Tamilnadu, INDIA-632006.*
[d]*Gopalan College of Engineering and Management, Bangalore, Karnataka, India, 560048.*

PAPER INFO

ABSTRACT

Magnetohydrodynamic application in the biomedical field made the researcher work more on this field in recent years. The major application of this concept is in scanning using laser beams, delivering a drug to the targeted points, cancer treatment, enhancing image contrast, etc. These applications are depending on the flow and heat transfer properties of the magnetic conducting fluid and on the geometry of the flow field. An increase in the demand for the miniature in the shape and size of the clinical devices attracts the researcher to work more on design optimization. In this study optimization of magnetic field strength, geometry of domain, Prandtl number, Reynolds number for a steady, incompressible double-diffusive flow is performed using Taguchi and Analysis of variance technique. Linear regression model is used to predict the average Nusselt and Sherwood numbers. Numerical simulations were performed using finite volume method (FVM) based numerical techniques. Experiments are designed based on Taguchi orthogonal array and FVM based numerical codes were used to obtain the results. Results show that an increase in the aspect ratio from to 0.5 to 2.0 improves the heat transfer rate by 62.0% and the mass transfer rate by 38.5%. As the Prandtl number increases from 0.7 to 13.0, heat transfer rate increases by 80.0% and mass transfer by 75.0%. This specific study could be applied in designing of solar ponds and to investigate heat and mass transfer effects during cancer treatments.

1. Introduction

Double diffusive mixed convection is widely used in many industrial and medical applications like solar ponds, material processing, Drug delivery systems, cancer treatments, solar air conditioning, packaging of electronic items, food processing, etc. Considering the wide application of double-diffusive mixed convection in the industrial and medical areas, further study is required to optimize the parameter influencing heat and mass transfer for maximum performance. Several numerical studies have been performed for the optimization of heat and mass transfer of the cavity flow. Rodrigues et al. [1] performed optimization of the geometry of the lid-driven cavity with two fins inside the cavity for mixed-type convection. They found that the asymmetric geometry of the fin plays a major role in controlling the temperature. Baag et al. [2] numerically studied the MHD effect using micropolar-type fluid flow on a vertical surface. They found that backflow is controlled by opposing buoyancy parameters. Khader and Megahed [3] used the Finite Difference Method to analyze the heat transfer on a liquid thin film over a stretching sheet using a numerical method. Li et al. [4] performed optimization

*Corresponding Author: Satheesh Anbalagan
Email: satheesh.a@vit.ac.in;egsatheesh@gmail.com

of nanoparticle size and other parameters on natural convection. They found that aspect ratio and Rayleigh number are the most significant parameters to control the thermal performance of the cavity. Iyi and Hasan [5] numerically performed the analysis on the effect of moistness using the buoyancy-driven flow of turbulence nature in a cavity. Li, et al. [6] have numerically optimized heat transfer in a microchannel using the field synergy principle. They found that internal cavity configuration plays a major role in controlling heat transfer. Mohammadi et al. [7] have optimized the heat transfer of flow of nanofluid inside a coil using Taguchi analysis. They found an optimum combination of a selected parameter for maximum performance. Srinivas, et al. [8] analyzed chemical reactions and thermal diffusion effect using MHD flow in a porous channel. The effect of different dimensional numbers has been considered in this analysis. Nath and Krishnan [9] performed an optimization analysis using Taguchi and the utility method of a double-diffusive type of flow using a channel filled with nanofluid. They compared the results of those methods and found that the utility method predicts marginally less Nu and Sh. Raei [10] used a Taguchi method for optimizing the heat exchanger operating with aluminum oxide nanofluid.Kishore, et al. [11] have done an optimization analysis of thermal electric generators using the Analysis of Variance (ANOVA) and the Taguchi method. They compared Taguchi and full factorial ANOVA results and found an 11.8% deviation. Iftikha et al. [12] performed a study on natural convective heat and mass transfer with inclined MHD effect using fractional operators. Hatami et al. [13] performed an optimization analysis of heat transfer using natural convection in a circular cavity. The results of their findings are, the Lewis number plays a major role in controlling the Nusselt number. Optimization of the cooled condenser for forced convection is performed by Kumara et al. [14]. The results of the Taguchi method show that improved performance is observed for 2-4 tubes kept at a 3-5 mm gap. Mamourian et al. [15] have optimized heat transfer by mixed convection and generation of entropy in a lid-driven cavity using the Taguchi method. They found the value of the optimum percentage of nanoparticles, wavelength, and Richardson number for better thermal performance of the cavity. Shirvan et al. [16] have numerically investigated and optimized the parameters involved in mixed convection using nanofluid flow in a cavity. The PISO algorithm is used to optimize the position of the heat sink and source in a closed enclosure Soleimani et al., [17]. An optimal combination for better thermal performance of the cavity is presented in this work. Position of multiple heat source optimization in a cavity was performed by Madadi and Balaji [18], using ANN and genetic algorithm. The result shows that a combination of ANN and GA will reduce the

computational period. Paulo et al. [19] analyzed the mixed convection laminar flow in a domain where two openings as an inlet and outlet in the vertical walls. Alinejad and Esfahani [20] used the Taguchi design approach to optimize the mixed convection in an enclosure. Taguchi's analysis shows that all the selected parameters show a significant effect on output. An optimal level of the selected parameters is also presented in the work. Gorobets et al. [21] published a numerical study on heat transfer with hydrodynamics effect in small diameter tube bundles. Hatami et al. [22] used a T-shaped cavity filled with a porous material and nanofluid to analyze and optimize heat transfer. ANN and GA are used by Mathew and Hotta [23] for optimizing IC chip arrangements on SMPS for mixed convection heat transfer. Results of the work show that the hybrid arrangement of chips is more effective than ordinary methods. Pichandi and Anbalagan [24] used a 2D enclosure to analyze the fluid flow and heat transfer analysis with the sinusoidal wave. LBM method is used for the analysis. Mirzakhanlari et al. [25] performed a sensitivity analysis to improve mixed convection and to reduce the coefficient of drag of fluid flow in a cavity with a rotating cylinder. The result of the analysis gives the effective values to increase the mean Nusselt number and reduce the drag coefficient. Sensitivity analysis and optimization are performed by Pordanjani et al. [26] to find the magnetic field effect on convection and entropy generation of nanofluid flow in an inclined domain. They found that Bejan and generation of entropy enhance with an increase in the thermal source length. Behbahan et al. [27] investigated the effect of aspect ratio on the melting thermal characteristics of metal foam. Investigation shows that aspect ratio plays a major role in changing the phase of copper foam. Selimefendigil and Öztop [28] Performed MHD convection optimization in a trapezoidal domain filled with nanofluid. Sudhakar et al. [29] used the ANN method to optimize the heat source configuration in a duct under mixed convection. Results show that CNN gives more accurate and fast results than computational studies. Tassone et al. [30] conducted optimization and heat transfer analysis of the cooling system using MHD flow in a WCLL blanket. Yigit and Chakraborty [31] performed a numerical analysis to find the effect of boundary condition and aspect ratio using Bingham fluids. Their investigation concludes that buoyancy forces improve flow by increasing the Rayleigh number. Hamzah et al. [32] published a research work on the effect of MHD on natural convection considering nanoparticle fluid flow in a U-Shape cavity. Yang and Yeh [33] optimized arrays of fins in a channel for mixed-type convection. A correlation of the aspect ratios for the maximum performance for different inclination angles is proposed in this study. Numerical investigation of the mixed convection effect in a square lid-driven cavity

under the combined effects of thermal and mass diffusion is numerically investigated [34]. Izadi et al. [35] performed a numerical analysis to find the effect of heat source and cavity aspect ratio using a C-shaped cavity on natural convection. They found a linear relationship between Nu and the aspect ratio of the enclosure. Béghein et al. [36] performed a numerical study on double-diffusive convection using a rectangular cavity. Alsobaai [37] used optimized petroleum residue thermal cracking using a three-level factorial design. Sathiyamoorthi and Anbalagan [38] presented their numerical study on entropy generation in double-diffusive natural convection in a square enclosure with the presence of a rectangular block at the center. They found that an increase in the Rayleigh number significantly increases entropy generation. An increase in Hartmann number decreases total entropy generation. Aljabair et al. [39] published a research article on the mixed convection of nanofluid flow in a lid-driven domain of sinusoidal nature. Teamah [40] performed numerical analysis on double diffusion using the rectangular domain. Recently, Moolya and Satheesh [41,42] performed a numerical study on the effect of an inclined magnetic field on double-diffusive mixed convection by considering different inclination angles. In the study, it is found that the magnetic field has a negative impact and the inclination angle has a positive impact on heat and mass transfer. Further, the work is extended for finding the optimum combination of the selected parameter for maximum performance. In the analysis, it is found that the Richardson number is the least significant parameter compared to all the selected parameters. Hasan et al. [43] used a mechanical chamber of triangular shape to analyze the periodic natural convection effect using CNT nanofluid. Raju et al. [44] performed a study on heat transmission and flow characteristics of nanofluid in a radiated flexible porous channel. They found that the distribution of temperature is higher in case-1, but the opposite finding is observed in a momentum boundary layer. Hossain et al [45] conducted a numerical study on the MHD convection effect using nanofluid with radiation. This analysis would help in designing thermal devices that work on nanofluids. Priyadharshini et al. [46] investigated the use of heat and mass transfer in MHD flow over a stretching sheet using a machine learning technique. They found that machine learning technology reduces the cost of simulation in the analysis of metal flow in metallurgy. Azad et al. [47] performed numerical analysis on heat and mass transfer properties in an enclosure using variable buoyancy ratio. Results show that an increase in the dimensionless time supports heat and mass transfer. Kavya et al. [48] used a stretching cylinder to study the magnetic-hybrid nanoparticle effect suspended in Cu nanoparticles. Their major finding is magnetic field reduces fluid velocity. Farahani [58] conducted an efficacy study on the magnetic field effect on heat transfer using nanofluid in a flattened tube with nanofluid. Senejani and Baniamerian [59] performed an optimization study of shell and tube heat exchangers using genetic, particle swarm, and Jaya optimization algorithms. Based on the above literature study, it is concluded that optimization of the geometry of the cavity and other related parameters to enhance the thermal performance of the cavity is needed to study further for better accuracy in the relevant field. Above mentioned literature it is found that aspect ratio also plays a major role in the present work, the aspect ratio is also considered one of the parameters. Also, by considering the importance of the Richardson number, it cannot be neglected without further investigation which was found as an insignificant parameter in the preceding study [41]. Therefore, to find the importance of the natural and forced convection effect, Grashof and Reynolds numbers are introduced. Hence in the present study, a two-dimensional domain, double-diffusive mixed convective laminar incompressible flow with MHD effect is considered. The performance of the cavity is determined by comparing Nusselt and Sherwood numbers for a different combination of dimensionless numbers. FVM-based numerical codes are used for the analysis and optimization is carried out using the Taguchi approach. The best combination of different dimensional numbers and the aspect ratio for maximum performance is obtained from the analysis. Residual plots obtained from linear regression models are used to correlate the fitted values with the observed values to check the accuracy of the obtained results. Following are the novelties of this study

- Analysis of the effect of nonlinear MHD effect on double-diffusive mixed convection by considering different aspect ratios
- The impact of thermal and momentum diffusivity on the heat transfer property of the cavity is analyzed
- A most significant parameter which controls the heat and mass transfer rate is analyzed
- An optimum combination of the selected parameter to maximize the rate of heat and mass transfer is determined by optimization analysis.
- Prediction models are developed.template, created in Microsoft Word 2013. Margins, column widths, line spacing, and type styles are built-in throughout this document. Author can use this document as a template and simply type own text into it.

2. Problem description and governing equations

A horizontal two-dimensional cavity model selected in this study is shown in Figure 1. The aspect ratio (L/H) is varied from 0.5 to 2.0 for the analysis. A horizontal magnetic field (Bo) is induced to the cavity

in a horizontal direction. Vertical sides of the cavity are kept with zero temperature and concentration gradients. Maximum temperature and concentration are kept to the top and bottom walls of the cavity. The upper wall is made to move towards positive x-direction to give a force convection effect and all other walls are kept stationary. The Newtonian and incompressible fluid is assumed for the analysis. All the thermal and physical properties of the fluid are assumed as constant except the density term. The variation of density term in the buoyancy force is calculated using a model developed by Boussinesq as shown in equation 1.

$$\rho = \rho_0[1 - \beta_T(T - T_c) - \beta_c(c - c_c)]. \qquad (1)$$

$$\beta_T = -\frac{1}{\rho_o}\left(\frac{\partial \rho}{\partial T}\right)_{P,c}; \qquad \beta_c = -\frac{1}{\rho_o}\left(\frac{\partial \rho}{\partial c}\right)_{P,T}. \qquad (2)$$

where βc is the concentration volumetric coefficient of expansion and βT is the thermal volumetric coefficient of expansion. The equations shown below are the governing equations used for flow, heat, and mass transfer respectively.

$$\frac{\partial u}{\partial x} + \frac{\partial v}{\partial y} = 0 \qquad (3)$$

$$u\frac{\partial u}{\partial x} + v\frac{\partial u}{\partial y} = -\frac{1}{\rho}\frac{\partial p}{\partial x} + \nu\left(\frac{\partial^2 u}{\partial x^2} + \frac{\partial^2 u}{\partial y^2}\right) \qquad (4)$$

$$u\frac{\partial v}{\partial x} + v\frac{\partial v}{\partial y} = -\frac{1}{\rho}\frac{\partial p}{\partial y} + \nu\left(\frac{\partial^2 v}{\partial x^2} + \frac{\partial^2 v}{\partial y^2}\right) \\ + g\,[\beta_T(T - T_c) \qquad (5) \\ + \beta_c(c - c_c)] + \frac{B_o^2\sigma}{\rho}v$$

$$u\frac{\partial T}{\partial x} + v\frac{\partial T}{\partial y} = \alpha\left(\frac{\partial^2 T}{\partial x^2} + \frac{\partial^2 T}{\partial y^2}\right) \qquad (6)$$

$$u\frac{\partial c}{\partial x} + v\frac{\partial c}{\partial y} = D\left(\frac{\partial^2 c}{\partial x^2} + \frac{\partial^2 c}{\partial y^2}\right). \qquad (7)$$

here, ν (kinematic viscosity), ρ (density), α (thermal diffusivity), Bo (magnetic induction), σ (electrical conductivity), and D (mass diffusivity) respectively. The dimensionless form of the equations mentioned above is written as follows:

$$X = \frac{x}{L}; \qquad Y = \frac{y}{L}; \qquad U = \frac{u}{U_{max}};$$

$$V = \frac{v}{U_{max}}; \qquad \theta = \frac{T - T_c}{T_h - T_c}; \qquad C = \frac{c - c_c}{c_h - c_c};$$

$$P = \frac{p}{\rho U_{max}^2}$$

Equations from (3) to (7) are written in the dimensionless form using the above dimensionless group.
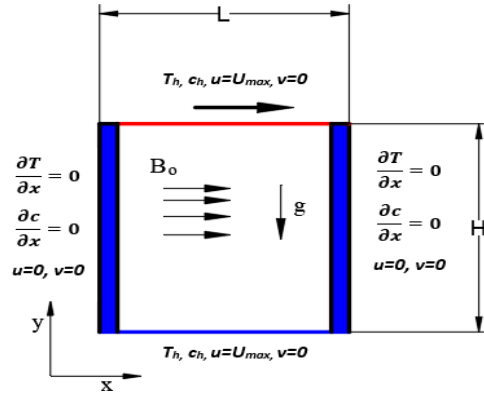
Figure 1. Schematic demonstration of the present problem

$$\frac{\partial U}{\partial X} + \frac{\partial V}{\partial Y} = 0 \qquad (8)$$

$$U\frac{\partial U}{\partial X} + V\frac{\partial U}{\partial Y} = -\frac{\partial P}{\partial X} + \frac{1}{Re}\left(\frac{\partial^2 U}{\partial X^2} + \frac{\partial^2 U}{\partial Y^2}\right) \qquad (9)$$

$$U\frac{\partial V}{\partial X} + V\frac{\partial V}{\partial Y} = -\frac{\partial P}{\partial Y} + \frac{1}{Re}\left(\frac{\partial^2 V}{\partial X^2} + \frac{\partial^2 V}{\partial Y^2}\right) \\ + Ri(\theta + NC) + \frac{Ha^2}{Re}V \qquad (10)$$

$$U\frac{\partial \theta}{\partial X} + V\frac{\partial \theta}{\partial Y} = \frac{1}{Re\,Pr}\left(\frac{\partial^2 \theta}{\partial X^2} + \frac{\partial^2 \theta}{\partial Y^2}\right) \qquad (11)$$

$$U\frac{\partial C}{\partial X} + V\frac{\partial C}{\partial Y} = \frac{1}{Re\,Sc}\left(\frac{\partial^2 C}{\partial X^2} + \frac{\partial^2 C}{\partial Y^2}\right) \qquad (12)$$

1. Reynolds number (Re)	:	$\dfrac{U_{max}L}{\nu}$
2. Richardson number (Ri)	:	$\dfrac{Gr_T}{Re^2}$
3. Buoyancy ratio (N)	:	$\dfrac{\beta_c(c_h - c_c)}{\beta_T(T_h - T_c)} = \dfrac{Gr_c}{Gr_T}$
4. Hartmann number (Ha)	:	$B_o L\sqrt{\dfrac{\sigma}{\rho U_{max}^2}}$
5. Prandtl number (Pr)	:	$\dfrac{\nu}{\alpha}$
6. Schmidt number (Sc)	:	$\dfrac{\nu}{D}$
7. Thermal Grashof number (Gr_T)	:	$\dfrac{g\beta_T(T_h - T_c)L^3}{\nu^2}$
8. solutal Grashof number (Gr_c)	:	$\dfrac{g\beta_c(c_h - c_c)L^3}{\nu^2}$

Following are the boundary condition of the problem selected,

Upper wall: $u = U_{max}; v = 0; T = T_h; c = c_h$

Lower wall: $u = v = 0; T = T_c; c = c_c$

Left and Right walls: $u = v = 0; \frac{\partial T}{\partial x} = \frac{\partial C}{\partial x} = 0$

3. Numerical Solution

The discretization of governing equations was done by FVM using uniform grid sizes. Pressure-velocity coupling equations were solved using the SIMPLE algorithm technique derived by (50). Convection-diffusion terms are solved by a central difference scheme. Equations obtained after discretization was solved iteratively using C++ code. In this selected criterion the convergence of the solution for the equations is 10-7. Nusselt number and Sherwood number are used to analyze the behavior of flow and the thermal characteristics of the fluid inside the cavity. Convective heat and species transfer inside the cavity are analyzed using flow behavior. Local and average Nu and Sh of the cavity hot wall are calculated as follows:

$$Nu = -\left(\frac{\partial \theta}{\partial Y}\right)_{Y=H} ; \quad Nu_{avg} = \int_0^L NudX. \quad (13)$$

The following equations are used to calculate Local Sh and average Sh,

$$Sh = -\left(\frac{\partial C}{\partial Y}\right)_{Y=H} ; \quad Sh_{avg} = \int_0^L Sh\, dX. \quad (14)$$

4. Result and Discussion

4.1. Grid Independence Study and Validation of Codes

A rectangular domain is used for the grid study. Several computations for the average Nu and Sh were performed for the uniform structured grid size from 41×21 to 201×101. The aspect ratio (L/H) selected for the grid-independent analysis is 2.0, therefore the number of grid sizes in the x-axis is two times the y-axis. Results of the simulation show an error of 0.6385 between the grid size 41×21 and 81×41 in average Nu and 10.63 in average Sh, 0.7918 in average Nu, and 2.3226 in average Sh between grid size 81×41 and 121×61, 0.5901 in average Nu and 0.368 in average Sh between grid size 121×61 and 161×81, 0.3551 in average Nu and 0.0736 in average Sh between grid size 161×81 and 201×101 is observed. There is a marginal variation in error is observed for both average Nu and Sh when the grid size changes from 121×61 to 161×81. Therefore 121×61 grid size is used for further analysis. Temperature and streamline contours of the present study are compared with Ji, et al. [49] as shown in Figure 2, and found good agreement between both results. Table 1 presents the validation of codes for the average Nu and the literature results. Obtained results show an excellent match with the literature results.

(a) Temperature
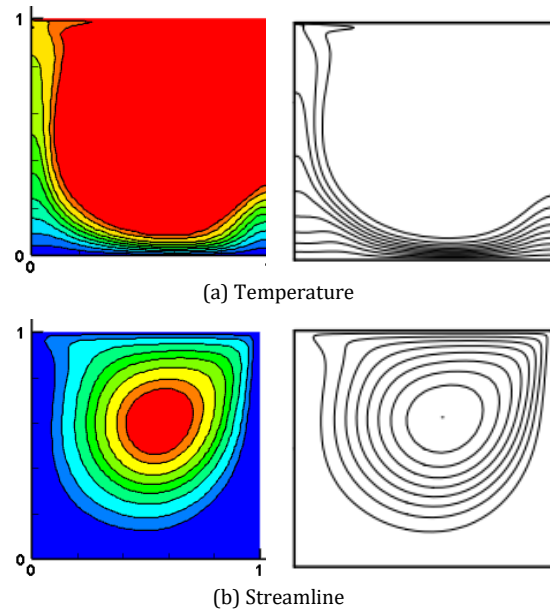
(b) Streamline

Figure 2. Comparison of (a) temperature and (b) streamline of the present study (left side) with Ji et al. [49] (right side)

Table 1. Comparison of avg. Nu of present work with the literature results for Grt=100, Pr=0.71 at different Re.

Literature	Re		
	100	400	1000
Present work	2.02	3.98	6.20
Hussain *et al.* [51]	2.03	4.07	6.58
Kefayati *et al.*[52]	2.09	4.08	6.54
Sheremet and Pop [53]	2.05	4.09	6.70
Sharif [54]	-	4.05	6.55
Iwatsu *et al.* [55]	1.94	3.84	6.33
Waheed [56])	2.03	4.02	6.48

4.2. Effect of the Magnetic Field, Prandtl number, and Aspect ratio

The temperature, concentration, and flow fields are shown below for different Ha, Pr, and aspect ratios. Thermal and concentration lines are orthogonal to the left and right walls since they are adiabatic walls. This ensures no heat and mass transfer through the walls. In streamline contour, a vertex is seen on the right portion of the domain due to the movement of the upper edge in the positive x-direction and the diffusion due to the buoyancy force. Figures 3(a), 3(b), and 3(c) show the variation of the contours of temperature, concentration, and streamlines for different Ha. The pattern of the contour plots indicates, the magnetic field greatly affects the temperature and concentration distribution inside the cavity. The negative effect is observed inside the cavity for both Nu and Sh as the value of Ha increases. This negative effect is mainly due to a decrease in the flow velocity due to the increase in the magnetic effect.

(a) Ha = 0

(b) Ha = 30

(c) Ha = 60
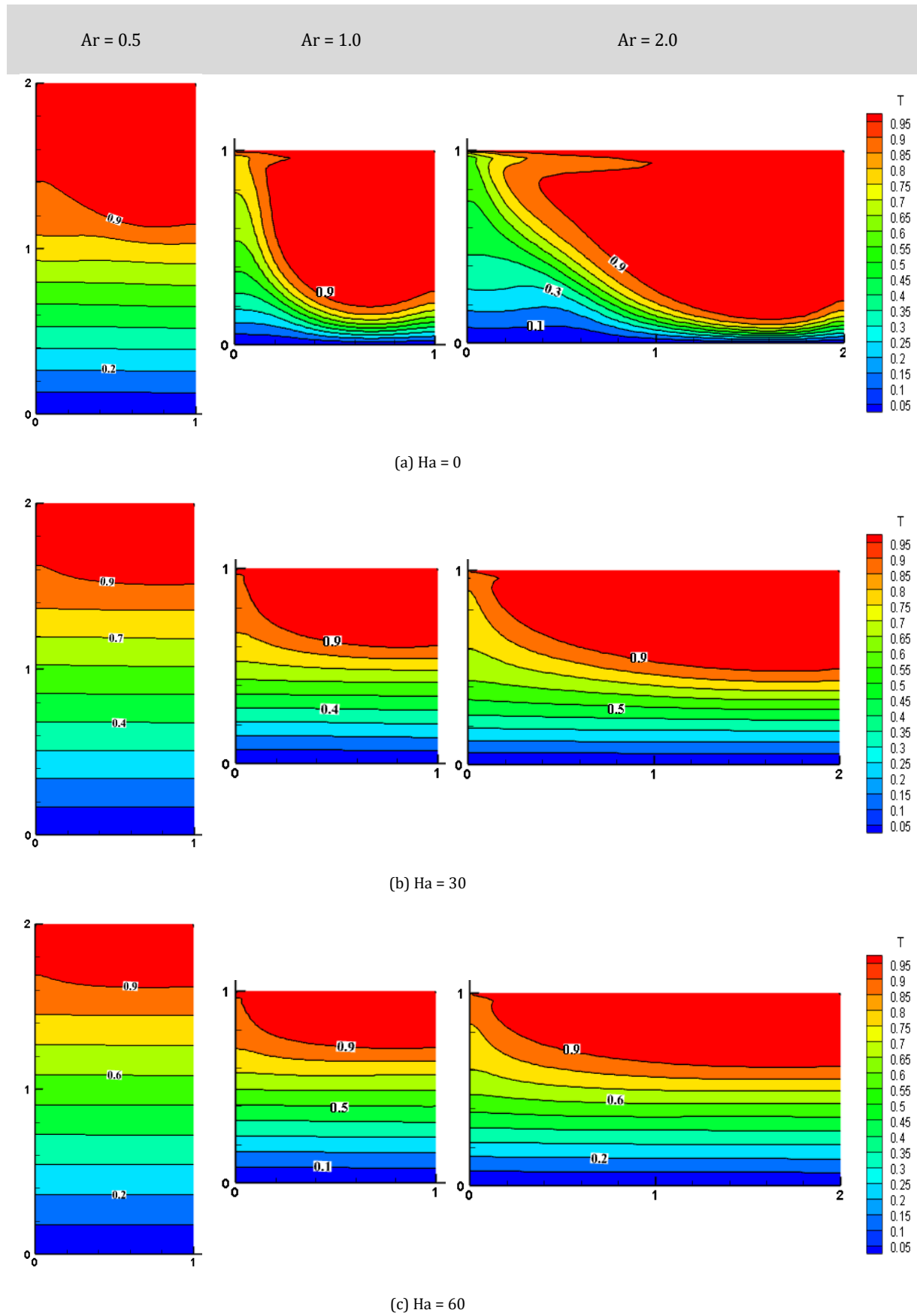
Figure 3 (a). Temperature contours at different Ha and Ar for Re = 100, Pr = 7.0, and Grt = 1000

Ar = 0.5   Ar = 1.0   Ar = 2.0

(a) Ha = 0

(b) Ha = 30

(c) Ha = 60
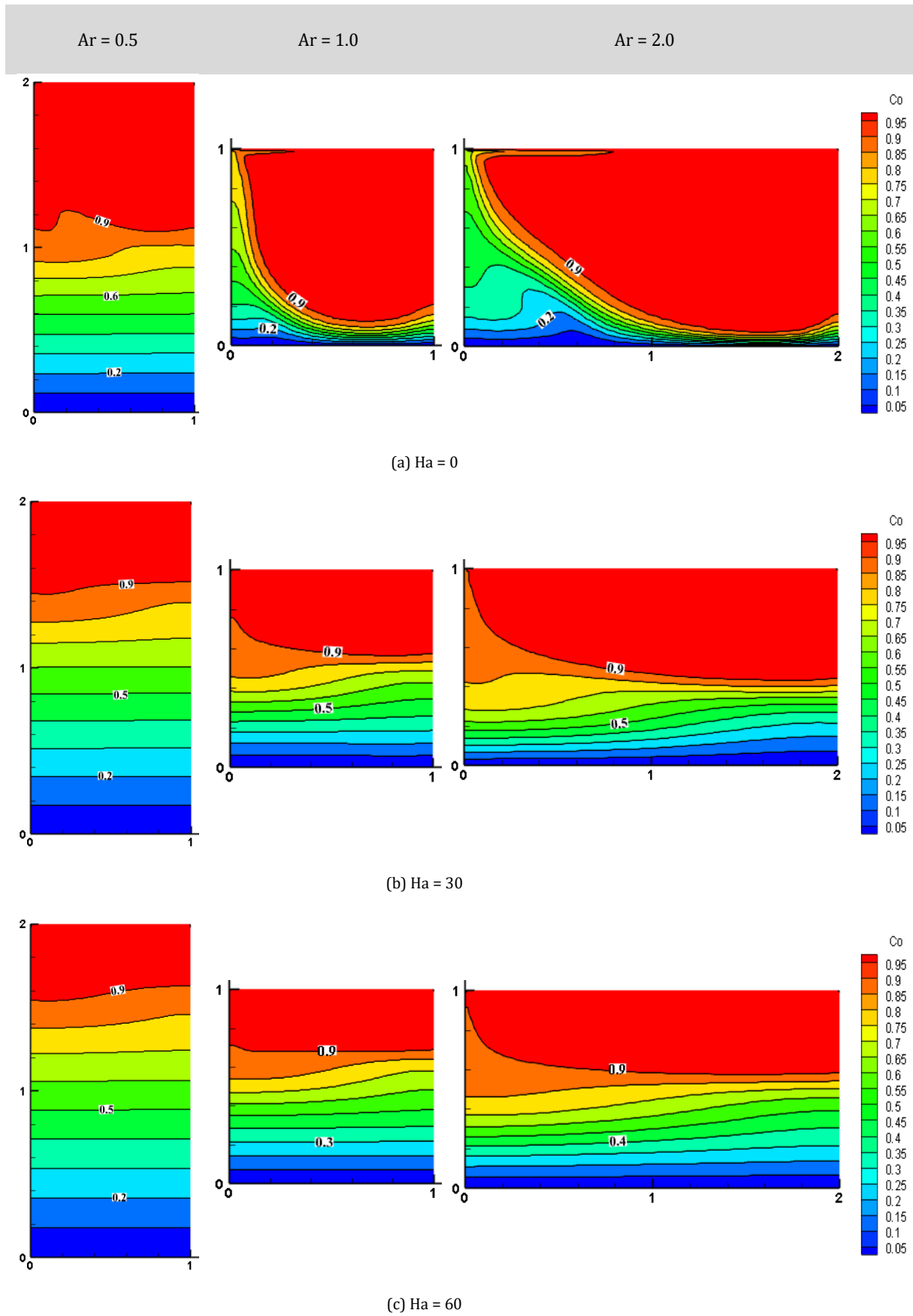
Figure 3 (b). Concentration contours at different Ha and Ar for Re = 100, Pr = 7.0, and Grt = 1000

(a) Ha = 0

(b) Ha = 30

(c) Ha = 60
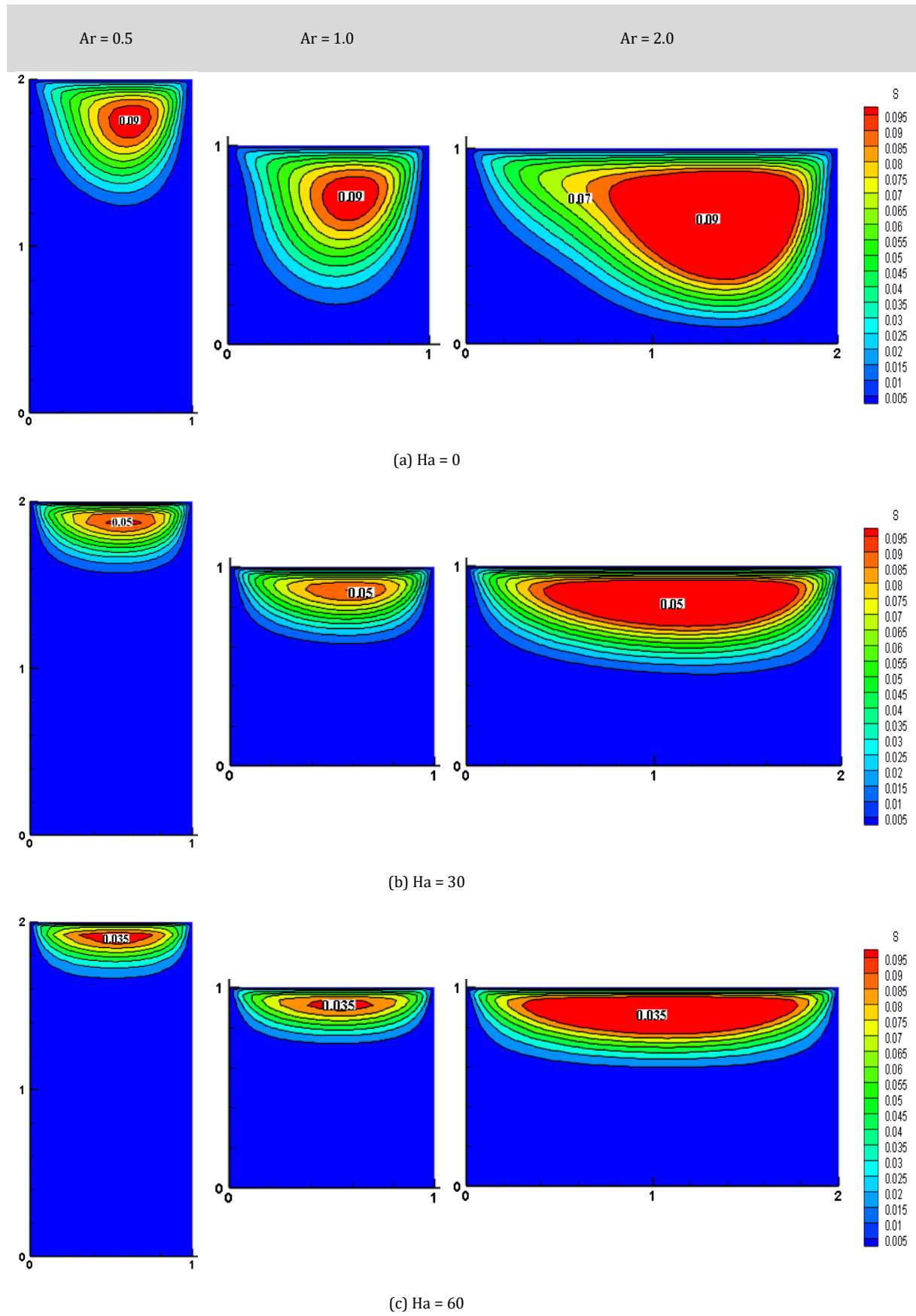
Figure 3 (c). Streamline contours at different Ha and Ar for Re = 100, Pr=7.0, and Grt=1000

Figures 4(a), 4(b), and 4(c) show the effect of Pr on the thermal performance of the cavity. More concentration and temperature distribution are observed as the value of Pr increases. An increase in the avg. Nu and Sh at the hot wall indicate improvement in the heat and mass transfer rate.

Compare to the thermal distribution, the magnitude of the concentration distribution is observed more because Le is maintained as 5. Not much change is observed in streamline contours because Ha is maintained as high and at the high magnetic field, flow velocity retards.

The effect of an aspect ratio of the cavity on heat and the species transfer rate is shown in Figure 5. Three different aspect ratios are taken for the analysis. Flow is observed as very weak for an aspect ratio less than one but increases for an aspect ratio greater than one. This is mainly due to an increase in the supply of heat at the top side of the cavity.

CFD analysis for the optimization of the performance of lid-driven cavity for heat and mass transfer has been performed by selecting the aspect ratio, thermal Grashof number, Reynolds number, Hartmann number and Prandtl number as the control parameters and average Nu and Sh are the responses.

Taguchi method of experimental design is used in this analysis for optimizing the performance of lid-driven cavities. In the following session, the method used for the present numerical analysis has been discussed.

4.3. Taguchi Method

Taguchi method is used to find the optimal combination of selected parameters for maximum performance of the domain in terms of average Nusselt and Sherwood numbers.

The parameters considered for the analysis are the cavity aspect ratio (Ar), Thermal Grashoff number (Gr), Reynold's number (Re), Hartmann number (Ha), and Prandtl number (Pr), and their level are shown in Table II.

Normally in the Taguchi method, L8, L16, L18, and L27 orthogonal arrays are used for parameter assignment. In this analysis, the L27 orthogonal array is considered which consists of 27 samples data shown in Table III.

The CFD codes were run as per Taguchi L27 combinations. The software used for the Taguchi analysis is Minitab 15.0.

The results of the Taguchi analysis and CFD simulation are shown in Table IV. Taguchi method reduces the number of experiments a researcher is required to perform which intern reduces the cost involved. The signal to Noise Ratio (S/N ratio) plot is used to discover the dominant level of the selected parameters.

The rank for each factor is assigned depending on the delta value obtained from the S/N ratio response table. The minimum rank in the table shows the maximum influence of factors on the output response. Five active parameters at three different levels were analyzed.

An optimal combination of levels of these factors for extreme performance of the domain is found. Graphs and contour plots are also used to investigate the heat and species transfer pattern in the cavity.

The present analysis uses L27 orthogonal with DOF 26. Five parameters and each parameter at 3 levels require $3^5 = 243$ experiments in a full factorial design, however, the Taguchi design requires only 27 runs which will reduce the time and cost.

Table 2. Levels of independent parameters

Independent Factors	Level-1	Level-2	Level-3
Ar	0.5	1	2
Grt	10^3	10^4	10^5
Re	100	500	1000
Ha	0	30	60
Pr	0.7	7	13

The S/N ratio is used to measure the variation in the Taguchi analysis method. The choice of the S/N ratio definition is based on the property response parameter or the characteristic value. Three different types of characteristic values are NB (Normal is the Best), SB (Smaller is the Best), and LB (Larger is the Better).

The main aim of the present analysis is to maximize the heat and mass transfer rate; therefore, LB is selected for the analysis. The S/N ratio calculated for the selected characteristic values is shown in Table IV and is calculated using the following expression, Eq. (15).

$$S/_N LB = -10log\left[\frac{1}{r}\sum_{j=1}^{r}\frac{1}{y_j^2}\right] \tag{15}$$

(a) Pr = 0.7

(b) Pr = 7.0

(c) Pr = 13.0
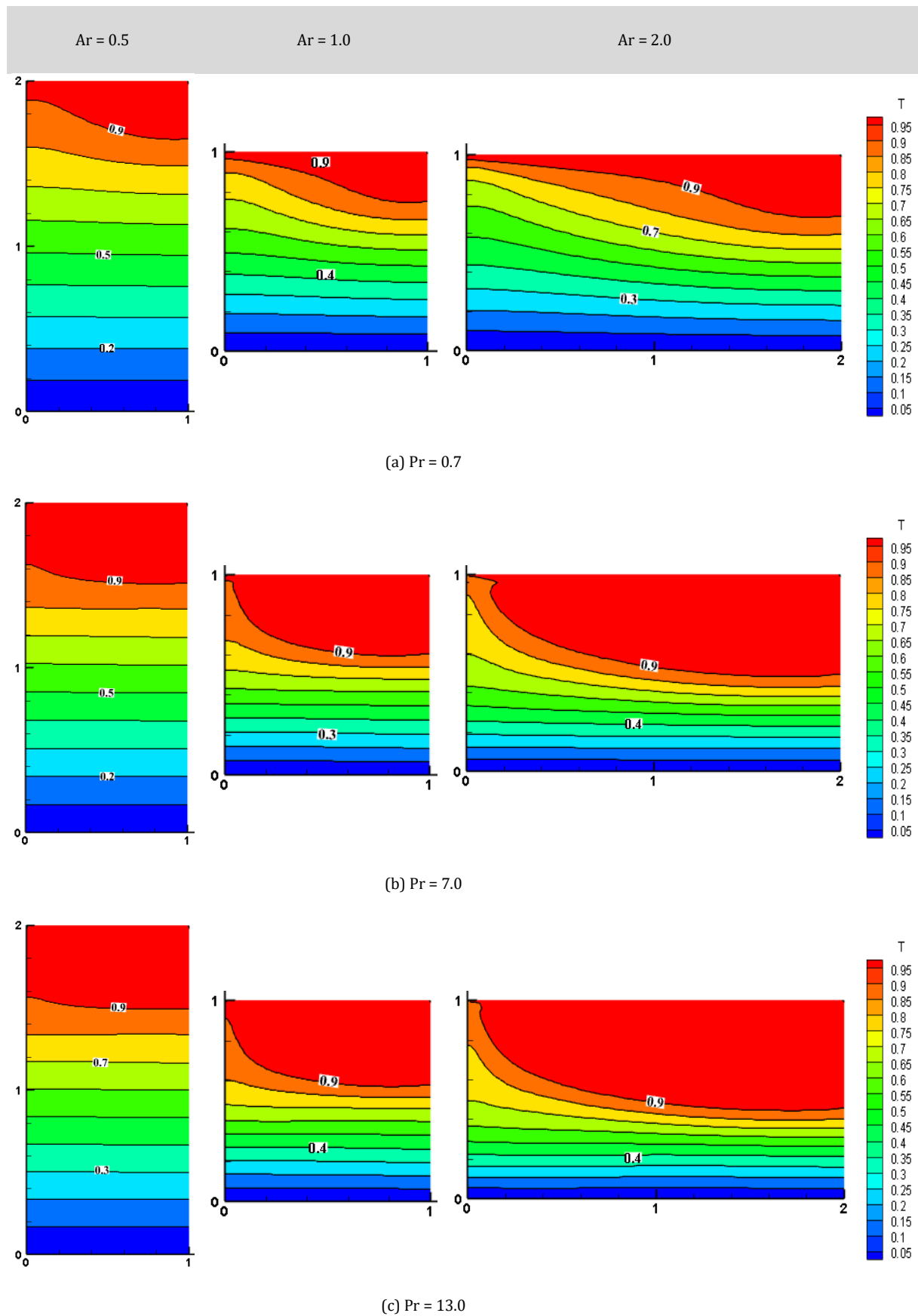
Figure 4 (a). Temperature contours at different Pr and Ar for Re = 100, Ha=0, and Grt=1000

(a) Pr = 0.7

(b) Pr = 7.0

(c) Pr = 13.0
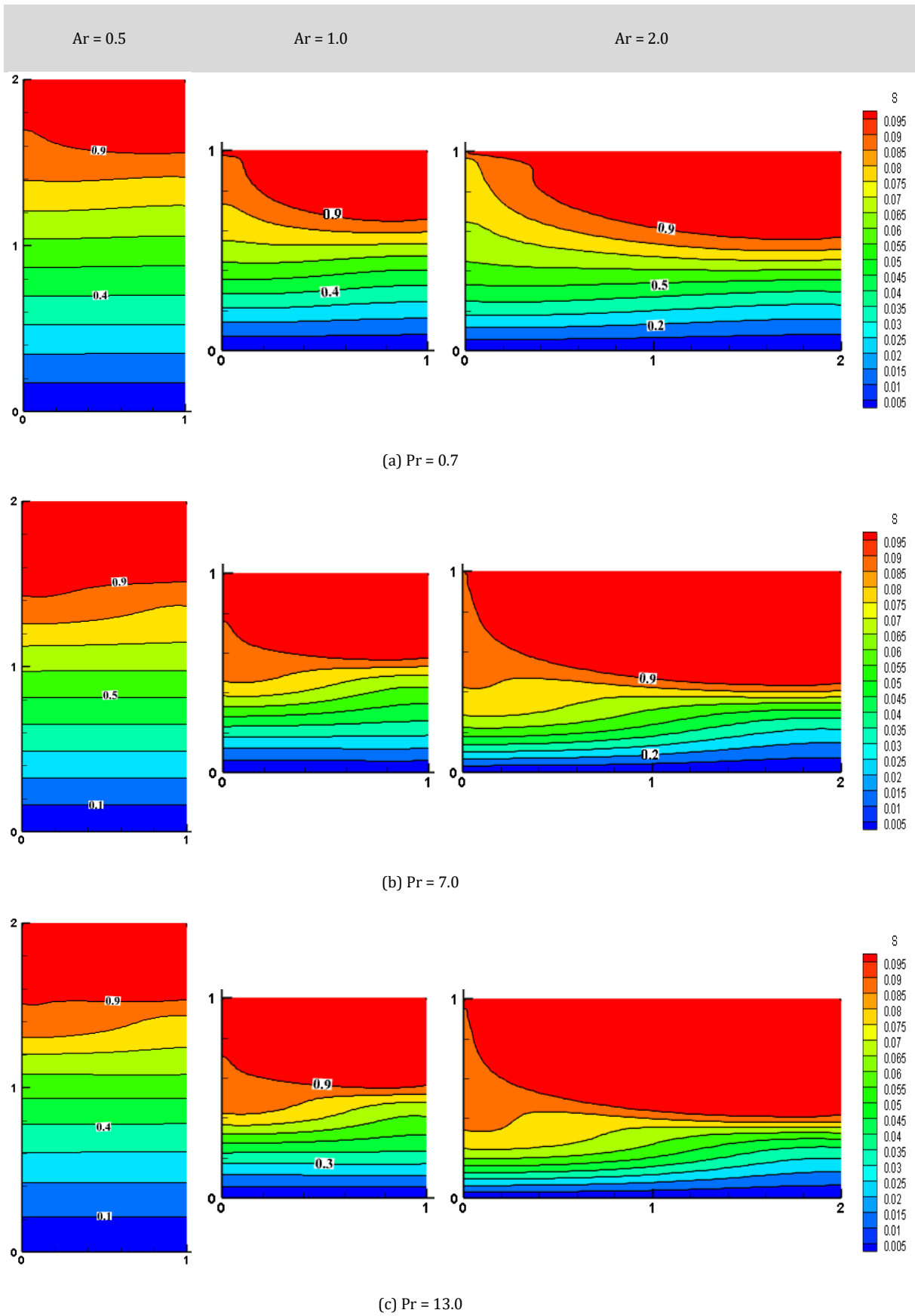
Figure 4 (b). Concentration at different Pr for Re = 100, Ha=0, and Grt=1000

(a) Pr = 0.7

(b) Pr = 7.0

(c) Pr = 13.0
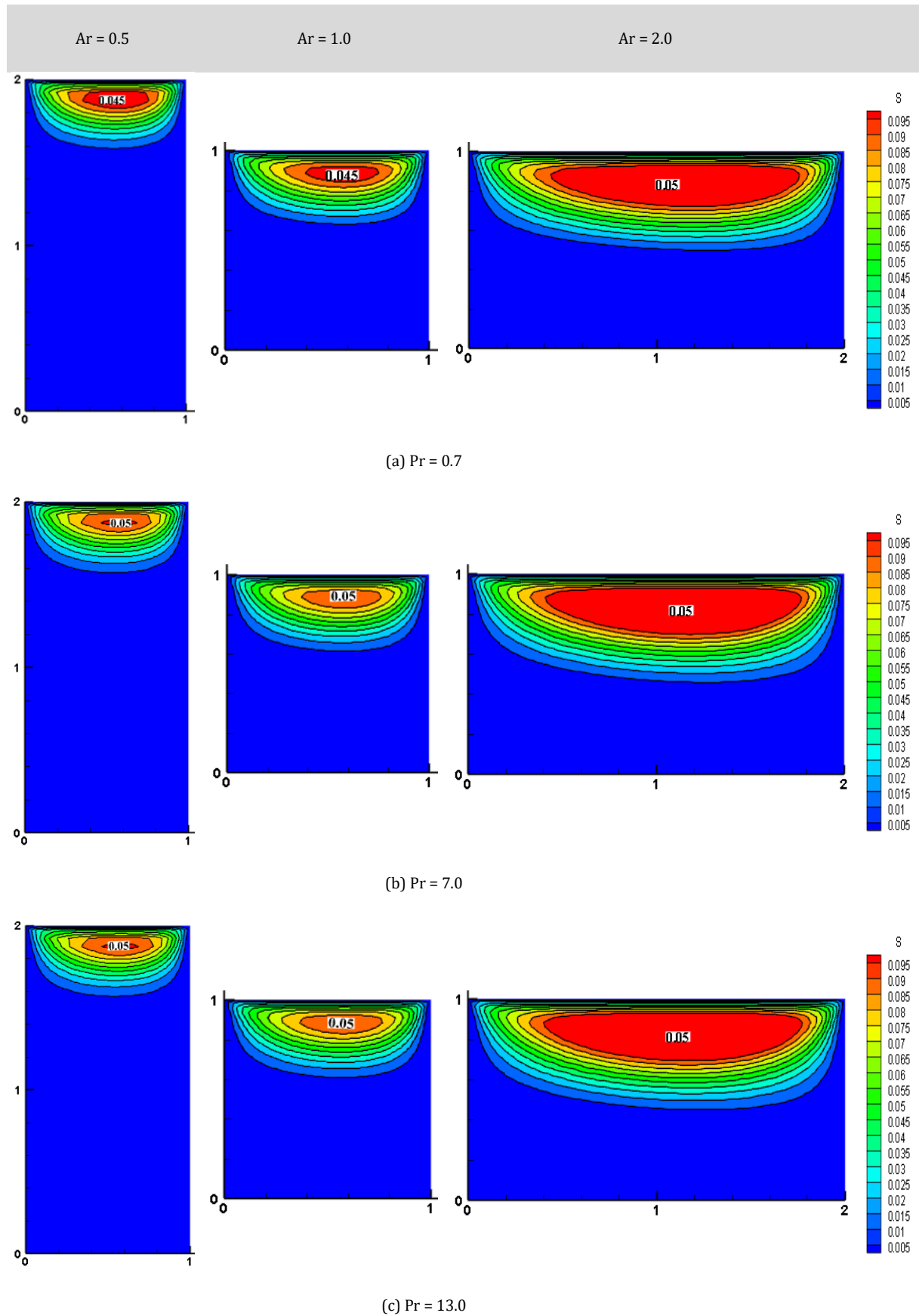
Figure 4 (c). Streamline contours at different Pr and Ar for Re = 100, Ha=0, and Grt=1000
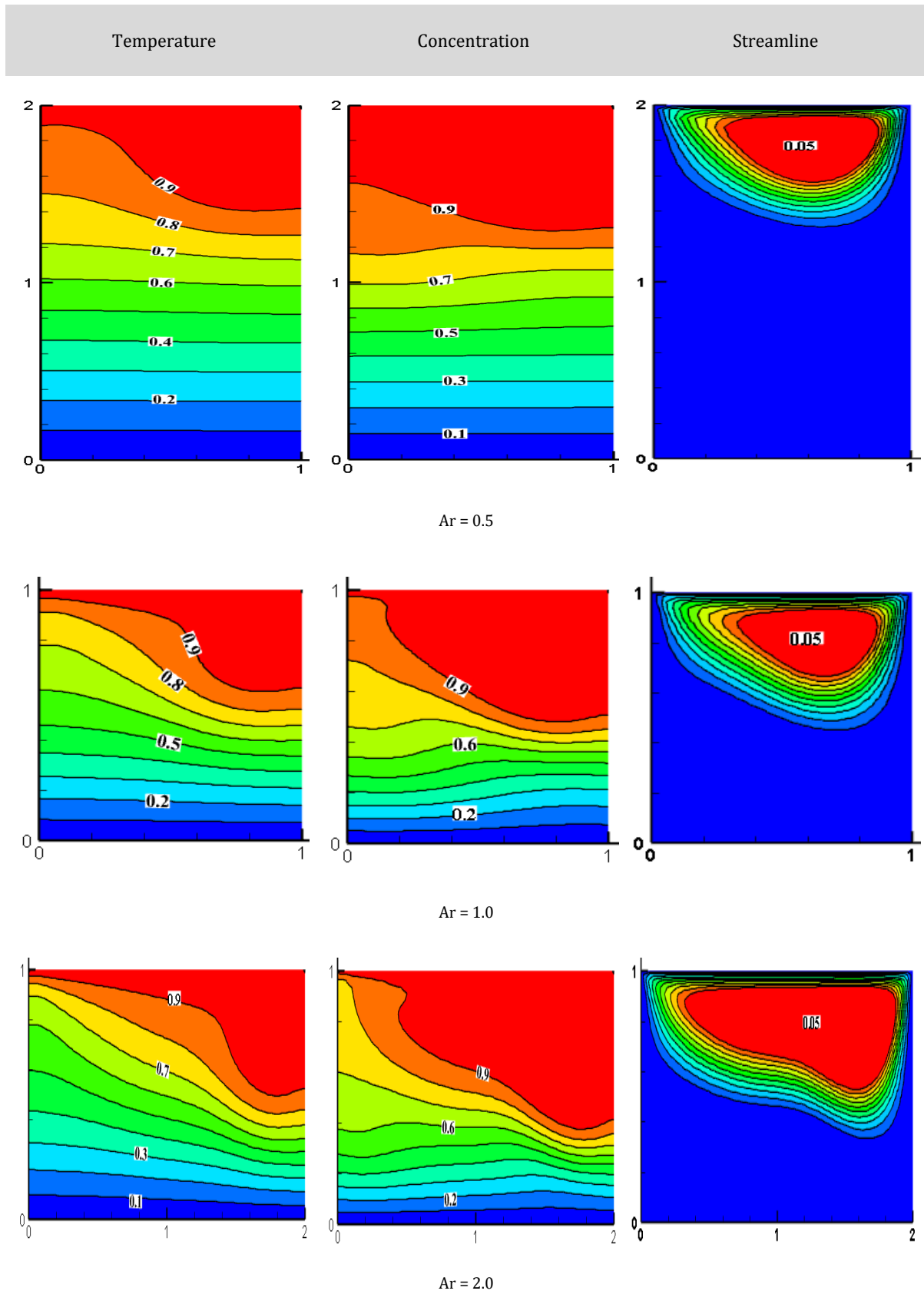
Figure 5. Temperature, Concentration and Streamline contours at different Ar for
Re = 100, Pr=0.7, Grt=1000 and Ha = 0

Table 3. L27 Taguchi orthogonal array table

Iteration No.	Factors				
	Ar	Grt	Re	Ha	Pr
1	0.5	1000	100	0	0.7
2	0.5	1000	100	0	7
3	0.5	1000	100	0	13
4	0.5	10000	500	30	0.7
5	0.5	10000	500	30	7
6	0.5	10000	500	30	13
7	0.5	100000	1000	60	0.7
8	0.5	100000	1000	60	7
9	0.5	100000	1000	60	13
10	1	1000	500	60	0.7
11	1	1000	500	60	7
12	1	1000	500	60	13
13	1	10000	1000	0	0.7
14	1	10000	1000	0	7
15	1	10000	1000	0	13
16	1	100000	100	30	0.7
17	1	100000	100	30	7
18	1	100000	100	30	13
19	2	1000	1000	30	0.7
20	2	1000	1000	30	7
21	2	1000	1000	30	13
22	2	10000	100	60	0.7
23	2	10000	100	60	7
24	2	10000	100	60	13
25	2	100000	500	0	0.7
26	2	100000	500	0	7
27	2	100000	500	0	13

Where y_j is the value of jth response data and r is the iteration number. The optimization of the selected parameters has been obtained by linking the Taguchi and ANOVA method. Figures 6 and 7 show the effect of independent variables on the average Nusselt and Sherwood numbers based on the S/N ratio. Steep variations of S/N ratios for Pr and Re indicate that these factors have the maximum influence to control the heat and mass transfer rates. As the aspect ratio increases the heat transfer rate also increases, this is mainly due to an increase in the length of the edge compared to height. The maximum value of 11.164 is found at level 3 of the aspect ratio and then the sharp reduction in the S/N ratio is found in other levels of Ar. The effect of the thermal Grashof number is the least preference to control the value of Nu and Sh is observed in the same graph. No difference in the value of S/N ratios of Nu and Sh is observed by varying the value of Ha from 30 to 60. As Reynold's number increases the heat and mass transfer rate also increases this is mainly because of the increase in the

mean velocity of the fluid. The effect of Ha and Grt in controlling the heat and mass transfer is comparatively less. Tables V and VI describe the rank of each parameter in controlling the thermal efficiency of the cavity. The order of significance is Pr, Re, Ar, Ha, and Grt in controlling both heat and mass transfer rates. The same pattern is observed in the S/N graph. Level 3 of Pr, Re, and Ar, and level 1 of Grt and Ha are the more significant levels. The corresponding values of the S/N ratio of average Nu are 12.040, 11.103, 11.164, 10.333, and 7.820 and similarly, the same order and level of significance are observed in controlling the mass transfer rate. The corresponding values of the S/N ratio of average Sh are 18.522, 14.080, 14.532, 12.229, and 13.527 respectively.
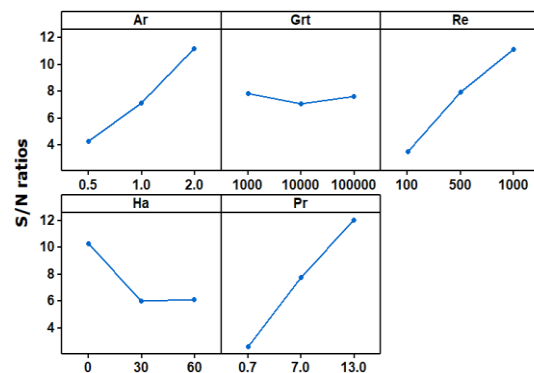
Figure 6. Graph of Independent variables effect on avg. Nu mean S/N ratios
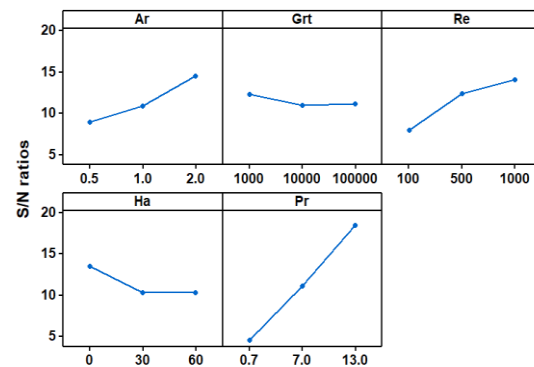
Figure 7. Graph of Independent variables effect on avg. Sh mean S/N ratios

4.4. Analysis of variance

The significance of different parameters to control heat and mass transfer in a lid-driven cavity is performed by adapting the method of analysis of variance (ANOVA). Five parameters at 3 levels have been considered for the analysis. The main purpose of this study is to find the finest arrangement of the selected factors to maximize the heat and species transfer rate. The significance of factors to control the thermal properties of the cavity is analyzed by taking a 95 % confidence level. The temperature and species transfer rates are analyzed using average Nu and Sh

values. Tables VII and VIII elucidate the significance and sum of squares of average Nu and Sh respectively. The contribution of each parameter to the total sum of squares (SS) is also seen in the same tables. This contribution percentage gives a clear idea about the importance of each factor in deciding the response. Using all those tables, a combination of parameters for optimal performance of the cavity can be easily predicted.

Table 4. S/N ratio table for average Nu and Sh

Trial No.	avg. Nu	S/N ratio	avg. Sh	S/N ratio
1	1.185	1.477	1.302	2.293
2	1.512	3.594	2.808	8.968
3	1.795	5.082	4.673	13.391
4	1.113	0.929	1.446	3.202
5	1.316	2.386	2.611	8.338
6	1.775	4.986	4.643	13.335
7	1.085	0.711	1.605	4.110
8	2.144	6.623	2.501	7.962
9	4.174	12.412	8.374	18.459
10	1.148	1.200	1.379	2.793
11	2.670	8.332	4.663	13.373
12	3.084	9.781	8.373	18.457
13	2.084	6.377	2.719	8.689
14	4.925	13.847	6.461	16.206
15	8.960	19.046	10.605	20.510
16	1.043	0.368	1.175	1.402
17	1.244	1.897	1.609	4.130
18	1.382	2.812	4.113	12.284
19	1.780	5.009	2.852	9.103
20	5.852	15.346	7.951	18.007
21	10.665	20.559	15.267	23.675
22	1.054	0.456	1.256	1.979
23	1.348	2.596	1.724	4.729
24	4.437	12.943	12.038	21.611
25	2.326	7.332	2.582	8.237
26	5.957	15.500	8.387	18.472
27	10.889	20.740	17.738	24.978

Table 5. Response table of S/N ratio on avg. Nu

Level	Ar	Grt	Re	Ha	Pr
1	4.244	7.820	3.469	10.333	2.651
2	7.073	7.063	7.910	6.032	7.791
3	11.164	7.599	11.103	6.117	12.040
Delta	6.920	0.757	7.634	4.300	9.389
Rank	3	5	2	4	1

Table 6. Response table of S/N ratio on avg. Sh

Level	Ar	Grt	Re	Ha	Pr
1	8.895	12.229	7.865	13.527	4.645
2	10.872	10.956	12.354	10.386	11.132
3	14.532	11.115	14.080	10.386	18.522
Delta	5.637	1.274	6.215	3.141	13.877
Rank	3	5	2	4	1

Table 7. ANOVA table for avg. Nu

Factors	DOF	(SS)	Variance	Value-F	Value-P	% Contribution
Ar	2	45.231	22.615	7.44	0.005	20.47
Grt	2	0.655	0.327	0.11	0.898	0.30
Re	2	39.764	19.882	6.54	0.008	18
Ha	2	20.412	10.206	3.36	0.061	9.24
Pr	2	66.228	33.114	10.90	0.001	29.98
Error	16	48.620	3.039	-	-	-
Total	26	220.910	-	-	-	100

Table 8 shows the analysis of variance for average Nu. From the P-value, it is clear that Pr, Ar, and Re are the significant factors to control the heat and mass transfer rate. The percentage contribution of Pr is more in both heat and mass transfer and which are 29.98% and 53% respectively. The contribution of Grt is comparatively very less in both cases; therefore, this parameter can be neglected for further analysis. The most optimal combination is Ar = 2.0, Grt =103, Re = 1000, Ha = 0 and Pr = 13.0. The residual plots were obtained by feeding the data obtained from the numerical studies into analytical software as shown in Figure 8 for average Nu and Figure 9 for average Sh. A normal distribution is observed in the residual plots indicating good agreement about the validity of the results (Joardar, Das, and Sutradhar, [57]). The normal probability plot shows the linear relationship which indicates error terms are distributed normally. The histogram of residuals indicates that residuals are distributed normally. From the above plots, it is clear that there is a good correlation between fitted values and the observed values.

The regression model equation for average Nu and Sh for the selected parameters is shown in equations 16 and 17. The standard error (S) of the average Nu regression model is found as 1.57and for the average Sh regression model is obtained as 2.32. The smaller values of S indicate that the model offers better fits due to minor residuals.

$$Avg\ Nu = -2.12+2.07Ar+0.000002Grt+0.00326Re-0.0343Ha+0.310Pr \qquad (16)$$

$$Avg\ Sh = -3.56+2.98Ar+0.000002\ Grt+0.00333Re-0.0284Ha+0.626Pr \qquad (17)$$

From these equations, it is clear that Ar, Grt, Re, and Pr have a positive impact on average Nu and average Sh, whereas Ha has a negative impact.

Table 8. ANOVA table for avg. Sh

Factors	DOF	(SS)	Variance	Value-F	Value-P	% Contribution
Ar	2	93.846	46.923	8.53	0.003	17.78
Grt	2	2.060	1.030	0.19	0.831	0.39
Re	2	46.392	23.196	4.22	0.034	8.79
Ha	2	17.766	8.883	1.61	0.230	3.36
Pr	2	279.705	139.853	25.42	0.000	53
Error	16	88.020	5.501	-	-	-
Total	26	527.788	-	-	-	100

4.5. Confirmation Test

A confirmation test was performed for the optimum combination. The simulations are performed using the optimal combination of Ar, Grt, Re, Ha, and Pr. The obtained results from this combination are compared with the results of all the simulations used in the analysis.

It is observed that the highest value of Nu and Sh is obtained in optimum combination. This confirms that the optimum combination is the best combination for maximizing heat and mass transfer.

The thermal, concentration, and flow fields for the optimal combination obtained from Taguchi and ANOVA results are offered in the form of isotherms, isoconcentration, and streamlines in Figure10.

The nature of the contours is perfectly validated with the obtained results. Considering the wide range of applications mentioned in the introduction section about the MHD flows and diffusion effect in controlling the thermal performance in medical and biomedical, power production, furnace design, and production of glass sheets, the present numerical results help to select the best combinations to improve the performance.

The value of average Nu and Sh obtained from the confirmation test for the optimal combination is 18.176 and 34.668 which clearly shows the highest values compare to all other combinations used in the analysis.
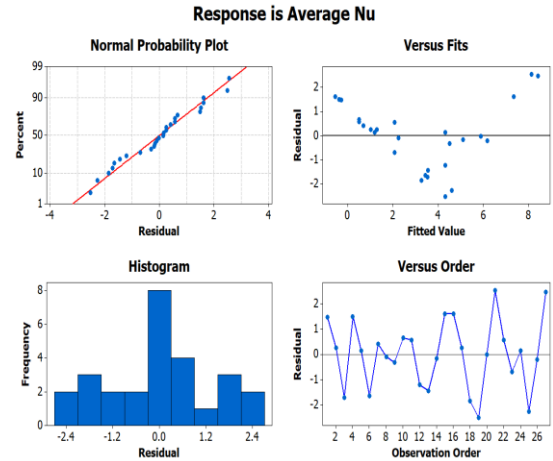
Figure 8. Average Nu residual plot
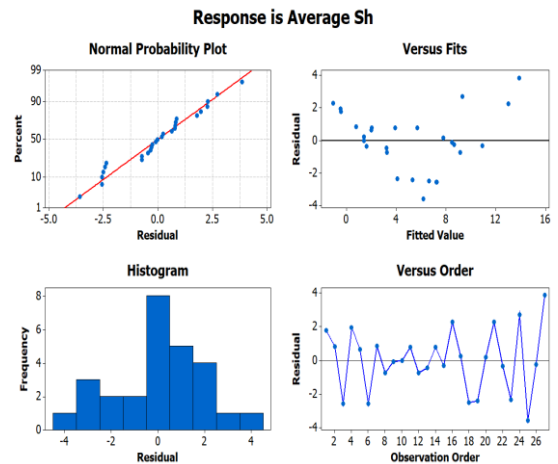
Figure 9. Average Sh residual plot

Temperature

Concentration
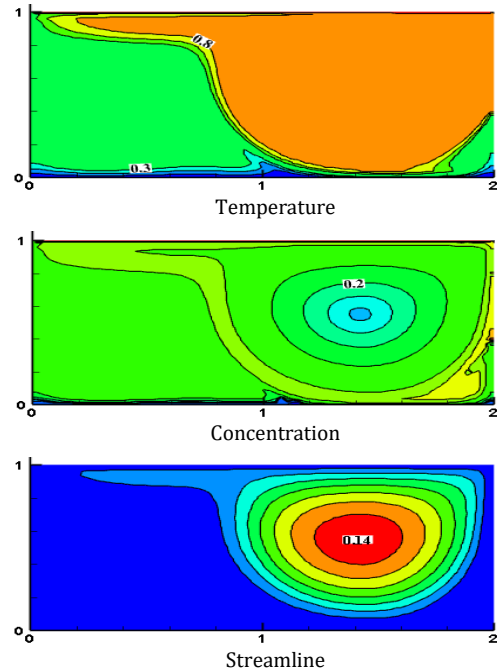
Streamline

Figure 10. Temperature, concentration and streamline contours at an optimized combination

Conclusion

In this work effect of different dimensionless numbers and their optimization for the supreme performance of the selected domain is numerically performed using a lid-driven cavity. The performance of the cavity is arbitrated using avg Nu and Sh values. The results obtained from the analysis are as follows.

- With an increase in Pr value to the third level, the heat transfer rate increases by 79.98%, and mass transfer by 74.92% which is the most significant parameter.
- Similarly, an increase in Re improves the heat transfer rate by 68.76% and the mass transfer rate by 44.140%. Re is the second significant parameter for the selected range of values.
- An increase in the aspect ratio improves the heat transfer rate by 61.98% and the mass transfer rate by 38.79%.
- The optimum level for the maximum performance of the cavity is obtained as Ar = 2.0, Grt = 103, Re = 1000, Ha = 0.0 and Pr = 13.0.
- The average Nu and Sh are dependent maximum on Pr, Re, and Ar and the effect of Grt and Ha are comparatively negligible.
- The value of average Nu and Sh obtained from the confirmation test for the optimal combination is 18.176 and 34.668 which clearly shows the highest values compare to all other combinations used in the analysis.
- The regression model shows a positive impact of all selected parameters on average Nu and Sh and a negative impact with Ha.

Nomenclature

Ar	Aspect ratio
Bo	Magnetic induction (tesla)
c	Concentration
C	Dimensionless concentration
D	Mass diffusivity(m2s-1)
g	Gravitational acceleration(ms-2)
GrC	Grashof number concentration
GrT	Grashof number temperature
h	Heat transfer coefficient($Wm^{-2}K^{-1}$)
hs	Solutal transfer coefficient(ms^{-1})
H	Enclosure height(m)
Ha	Hartmann number
L	Enclosure length(m)
Le	Lewis number
N	Buoyancy ratio
Nu	Nusselt number
p	Pressure(Nm^{-2})
P	Non-dimensional pressure
Pr	Prandtl number
Re	Reynolds number
Ri	Richardson number
Sc	Schmidt number
Sh	Sherwood number
T	Dimensional temperature(K)
u,v	Dimensional velocity component (ms-1)
U,V	Dimensionless velocity components
x,y	Dimensional co-ordinates
X,Y	Dimensionless Cartesian coordinates
r	Iteration number

Greek symbol

α	Thermal diffusivity(m^2s^{-1})
β	Fluid thermal expansion coefficient(K^{-1})
θ	Dimensionless temperature
ν	Effective kinematic viscosity(m^2s^{-1})
ρ	Density(kgm^{-3})
σ	Fluid electrical conductivity(sm^{-1})

Subscripts

avg	Average
C	Cold, Concentration
h	Hot
T	Thermal
max	Maximum

References

[1]. P.M. Rodrigues, C. Biserni, C.C. de Escobar, L.A.O. Rocha, L.A. Isoldi, E.D. dos Santosa, Geometric optimization of a lid-driven cavity with two rectangular intrusions under mixed convection heat transfer: A numerical investigation motivated by constructal design, International Communications in Heat and Mass Transfer, 117, 104759, (2020)

[2]. S. Baag, S.R. Mishra, G.C. Dash, M.R.Acharya, Numerical investigation on MHD micropolar fluid flow toward a stagnation point on a vertical surface with heat source and chemical reaction, Journal of King Saud University - Engineering Sciences, 29(1), 75–83, (2017).

[3]. M.M. Khader, and A.M. Megahed, Numerical simulation using the finite difference method for the flow and heat transfer in a thin liquid film over an unsteady stretching sheet in a saturated porous medium in the presence of thermal radiation, Journal of King Saud University - Engineering Sciences, 25(1), 29–34, (2013).

[4]. Z. Li, A.K. Hussein, O.Younis, S.Rostami, W. He, Effect of alumina nano-powder on the natural convection of water under the influence of a magnetic field in a cavity and optimization using RMS: Using empirical correlations for the thermal conductivity and a sensitivity analysis, International Communications in Heat and Mass Transfer, 112, 104497, (2020).

[5]. D. Iyi, and R. Hasan, Numerical investigation of the effect of moisture on buoyancy-driven low turbulence flow in an enclosed cavity, International Journal of Heat and Mass Transfer, 136, 543–554, (2019).

[6]. F. Li, W. Zhu, and H. He, Numerical optimization on microchannel flow and heat transfer performance based on field synergy principle, International Journal of Heat and Mass Transfer, 130, 375–385, (2019).

[7]. M. Mohammadi, A. A, Reza, N. Farouji, M.P. Fard, An optimization of heat transfer of nanofluid flow in a helically coiled pipe using Taguchi method, Journal of Thermal Analysis and Calorimetry, 138(2), 1779–1792, (2019).

[8]. S. Srinivas, T. Malathy, A.S. Reddy, A note on thermal-diffusion and chemical reaction effects on MHD pulsating flow in a porous channel with slip and convective boundary conditions, Journal of King Saud University - Engineering Sciences, 28(2), 213–221, (2016)

[9]. R. Nath and M. Krishnan, Optimization of double diffusive mixed convection in a BFS channel filled with Alumina nanoparticle using Taguchi method and utility concept, Scientific Reports, Springer US, 9(1), 1–19, (2019).

[10]. B. Raei, Statistical analysis of nanofluid heat transfer in a heat exchanger using Taguchi method, Journal of heat and mass transfer research, 8(1),29–38, (2021).

[11]. R. Kishore, A.M. Sanghadasa S. Priya, Optimization of segmented thermoelectric generator using Taguchi and ANOVA techniques, Scientific Reports. Springer US, 7(1), 1–15, (2017).

[12]. N. Iftikhar, D. Baleanu, M.B. Riaz, S. M. Husnine, Heat and mass transfer of natural convective flow with slanted magnetic field via fractional operators, Journal of Applied and Computational Mechanics, 7(1), 189–212, (2021).

[13]. M. Hatami, D. Song, D. Jing, Optimization of a circular-wavy cavity filled by nanofluid under the natural convection heat transfer condition, International Journal of Heat and Mass Transfer, 98, 758–767, (2016).

[14]. Kumara, J.B. Joshi, A.K. Nayak, P.K. Vijayan, 3D CFD simulations of air cooled condenser-III: Thermal-hydraulic characteristics and design optimization under forced convection conditions, International Journal of Heat and Mass Transfer, 93, 1227–1247, (2016).

[15]. M. Mamourian, K.M. Shirvan, R.Ellahi, A.B. Rahimia, Optimization of mixed convection heat transfer with entropy generation in a wavy surface square lid-driven cavity by means of Taguchi approach, International Journal of Heat and Mass Transfer, 102, 544–554, (2016).

[16]. K.M. Shirvan, K, M, M. Mamourian, R. Ellahi, Numerical investigation and optimization of mixed convection in ventilated square cavity filled with nanofluid of different inlet and outlet port, International Journal of Numerical Methods for Heat and Fluid Flow, 27(9), 2053–2069, (2017).

[17]. S. Soleimani, D.D. Ganji, M. Gorji, H.Bararnia, E.Ghasemi, Optimal location of a pair heat source-sink in an enclosed square cavity with natural convection through PSO algorithm, International Communications in Heat and Mass Transfer, 38(5), 652–658, (2011).

[18]. R.R. Madadi, and C. Balaji, Optimization of the location of multiple discrete heat sources in a ventilated cavity using artificial neural networks and micro genetic algorithm, International Journal of Heat and Mass Transfer, 51(9–10), 2299–2312, (2008).

[19]. M. Paulo, G. Menon, M.D. Ramos, Mixed convection study in a ventilated square cavity using nanofluids, Journal of heat and mass transfer research, 6(2), 143–153, (2019).

[20]. J. Alinejad and J.A. Esfahani, Taguchi design of three dimensional simulations for optimization of turbulent mixed convection in a cavity, Meccanica, 52(4–5), pp. 925–938, (2017).

[21]. V. Gorobets, V. Trokhaniak, Y. Bohdan, I. Antypov, Numerical Modeling of Heat Transfer and Hydrodynamics in Compact Shifted Arrangement Small Diameter Tube Bundles, Journal of Applied and Computational Mechanics, 7(1), pp. 292–301.

[22]. M.Hatami, J. Zhou, J. Geng, D. Song, D. Jing, Optimization of a lid-driven T-shaped porous cavity to improve the nanofluids mixed convection heat transfer, Journal of Molecular Liquids, 231, 620–631, (2017).

[23]. V.K. Mathew, and T.K. Hotta, Numerical investigation on optimal arrangement of IC chips mounted on a SMPS board cooled under mixed convection, Thermal Science and Engineering Progress, 7, 221–229, (2018).

[24]. P. Pichandi and S. Anbalagan, Natural convection heat transfer and fluid flow analysis in a 2D square enclosure with sinusoidal wave and different convection mechanism, International Journal of Numerical Methods for Heat and Fluid Flow, 28(9), 2158–2188, (2018).

[25]. S. Mirzakhanlari, K.M. Shirvan, M. Mamourian, Ali J.Chamkha, Increment of mixed convection heat transfer and decrement of drag coefficient in a lid-driven nanofluid-filled cavity with a conductive rotating circular cylinder at different horizontal locations: A sensitivity analysis, Powder Technology, 305, 495–508, (2017).

[26]. A.H. Pordanjani, S.M. Vahedi, S. Aghakhani, M. Afrand, H.F. Öztop, N.A. Hamdeh, Effect of magnetic field on mixed convection and entropy generation of hybrid nanofluid in an inclined enclosure: Sensitivity analysis and optimization, European Physical Journal Plus, 134(8), 412, (2019).

[27]. Behbahan, A. Noghrehabadi, C.P. Wong, I. Pop, M.B. Nejad, Investigation of enclosure aspect ratio effects on melting heat transfer characteristics of metal foam/phase change material composites, International Journal of Numerical Methods for Heat and Fluid Flow, 29(9), 2994–3011, (2019).

[28]. F. Selimefendigil and H.F. Öztop, Modeling and optimization of MHD mixed convection in a lid-driven trapezoidal cavity filled with alumina–water nanofluid: Effects of electrical conductivity models, International Journal of Mechanical Sciences. 136, 264–278, (2018).

[29]. T.V.V. Sudhakar, C. Balaji, S.P. Venkateshan, Optimal configuration of discrete heat sources in a vertical duct under conjugate mixed convection using artificial neural networks, International Journal of Thermal Sciences. 48(5), 881–890, (2009).

[30]. Tassone, MHD mixed convection flow in the WCLL: Heat transfer analysis and cooling system optimization, Fusion Engineering and Design, 146, 809–813, (2019).

[31]. S. Yigit and N. Chakraborty, Influences of aspect ratio and wall boundary condition on laminar Rayleigh-Bénard convection of Bingham fluids in rectangular enclosures, International Journal of Numerical Methods for Heat and Fluid Flow, 27(2), 310–333, (2017).

[32]. H. K. Hamzah, F.H. Ali, M. Hatami, D. Jing, Effect of Two Baffles on MHD Natural Convection in U-Shape Superposed by Solid Nanoparticle having Different Shapes, Journal of Applied and Computational Mechanics, 6, 1200–1209, (2020).

[33]. M.H. Yang and R.H. Yeh, Optimization of fin arrays in an inclined channel for mixed convection, Applied Thermal Engineering, 148(482), 963–976, (2019).

[34]. A.M. Al-Amiri, K.M. Khanafer, Numerical simulation of double-diffusive mixed convection within a rotating horizontal annulus, International Journal of Thermal Sciences, 45(6), 567–578, (2006).

[35]. M. Izadi, R. Mohebbi, A. Chamkha, I. Pop, Effects of cavity and heat source aspect ratios on natural convection of a nanofluid in a C-shaped cavity using Lattice Boltzmann method, International Journal of Numerical Methods for Heat and Fluid Flow, 28(8), 1930–1955, (2018).

[36]. C. Béghein, F. Haghighat, F. Allard, Numerical study of double-diffusive natural convection in a square cavity, International Journal of Heat and Mass Transfer, 35(4), 833–846, (1992).

[37]. A.M. Alsobaai, Thermal cracking of petroleum residue oil using three level factorial design, Journal of King Saud University - Engineering Sciences, 25(1), 21–28, (2013).

[38]. S. Arun, A. Satheesh, Mesoscopic analysis of heatline and massline during double-diffusive MHD natural convection in an inclined cavity, Chinese Journal of Physics. 56(5), 2155–2172, (2018).

[39]. S. Aljabair, A.L.Ekaid, S.H. Ibrahim, I. Alesbe, Heliyon Mixed convection in sinusoidal lid driven cavity with non-uniform temperature distribution on the wall utilizing nano fluid, Heliyon, 7, e06907, (2021).

[40]. M.A. Teamah, A.F. Elsafty, E.Z. Massoud, Numerical simulation of double-diffusive natural convective flow in an inclined rectangular enclosure in the presence of magnetic field and heat source, International Journal of Thermal Sciences, 52(1), 161–175, (2012).

[41]. S. Moolya, A. Satheesh, Role of magnetic field and cavity inclination on double diffusive mixed convection in rectangular enclosed domain, International Communications in Heat and Mass Transfer. 118, 104814, (2020).

[42]. S. Moolya, A. Satheesh, Optimization of the effect of Prandtl number, inclination angle, magnetic field, and Richardson number on double-diffusive mixed convection flow in a rectangular domain, International Communications in Heat and Mass Transfer, 126, 105358, (2021).

[43]. M. J. Hasan, A. K. Azad, Z. Islam, R. Hossain, and M. M. Rahman, "Periodic Unsteady Natural Convection on CNT Nano-powder Liquid in a Triangular Shaped Mechanical Chamber," Int. J. Thermofluids. 15, 100181, (2022)

[44]. C. S. K. Raju, N. A. Ahammad, K. Sajjan, N. A. Shah, S. J. Yook, and M. D. Kumar, "Nonlinear movements of axisymmetric ternary hybrid nanofluids in a thermally radiated expanding or contracting permeable Darcy Walls with different shapes and densities: Simple linear regression," Int. Commun. Heat Mass Transf., 135, 106110, (2022)

[45]. R. Hossain, A. K. Azad, M. J. Hasan, and M. M. Rahman, "Radiation effect on unsteady MHD mixed convection of kerosene oil-based CNT nanofluid using finite element analysis," Alexandria Eng. J. 61 (11) ,8525–8543, (2022)

[46]. P. Priyadharshini, M. V. Archana, N. A. Ahammad, C. S. K. Raju, S. jin Yook, and N. A. Shah, "Gradient descent machine learning regression for MHD flow: Metallurgy process," Int. Commun. Heat Mass Transf., 138, 106307, (2022).

[47]. A. K. Azad et al., "Numerical study on heat and mass transfer characteristics in a confined enclosure with variable buoyancy ratio," Results Eng., 15, 100569, (2022).

[48]. S. Kavya, V. Nagendramma, N. A. Ahammad, S. Ahmad, C. S. K. Raju, and N. A. Shah, "Magnetic-hybrid nanoparticles with stretching/shrinking cylinder in a suspension of MoS4 and copper

nanoparticles," Int. Commun. Heat Mass Transf., 136, 106150, (2022)

[49]. T.H. Ji, S.Y. Kim, J.M. Hyun, Transient mixed convection in an enclosure driven by a sliding lid, 629–638, (2007).

[50]. Suhas V. Patankar, Numerical Heat Transfer and Fluid Flow, Series in computational methods in mechanics and thermal sciences (1980).

[51]. S. Hussain, S.E. Ahmed, T. Akbar, Entropy generation analysis in MHD mixed convection of hybrid nanofluid in an open cavity with a horizontal channel containing an adiabatic obstacle, International Journal of Heat and Mass Transfer, 114, 1054–1066, (2017).

[52]. G.H.R. Kefayati, M.G. Bandpy, H. Sajjadi, D.D. Ganji, Lattice Boltzmann simulation of MHD mixed convection in a lid-driven square cavity with linearly heated wall, Scientia Iranica, 19(4), pp. 1053–1065, (2012).

[53]. M.A. Sheremet, I. Pop, Mixed convection in a lid-driven square cavity filled by a nanofluid: Buongiorno's mathematical model, Applied Mathematics and Computation, 266, 792–808, (2015).

[54]. M.A.R. Sharif, Laminar mixed convection in shallow inclined driven cavities with hot moving lid on top and cooled from bottom, Applied Thermal Engineering, 27(5–6), 1036–1042, (2007).

[55]. R. Iwatsu, J.M. Hyun, K. Kuwahara, Mixed convection in a driven cavity with a stable vertical temperature gradient, International Journal of Heat and Mass Transfer, 36(6), 1601–1608, (1993).

[56]. M. A. Waheed, Mixed convective heat transfer in rectangular enclosures driven by a continuously moving horizontal plate, International Journal of Heat and Mass Transfer, 52(21–22), 5055–5063, (2009).

[57]. H. Joardar, N. Das, G. Sutradhar, An experimental study of effect of process parameters in turning of LM6/SiCP metal matrix composite and its prediction using response surface methodology, International Journal of Engineering, Science and Technology, 3(8), 132–141, (2012).

[58]. S. D. Farahani, Efficacy of Magnetic Field on Heat Transfer of Nanofluid Flow in Flatten Tube with Porous Medium, J. Heat Mass Transf. Res., 9, 99–106, (2022).

[59]. A. K. Senejani and Z. Baniamerian, Multi Objective Optimization of Shell & Tube Heat Exchanger by Genetic, Particle Swarm and Jaya Optimization Algorithms: Assessment of Nanofluids as the Coolant, J. Heat Mass Transf. Res., 9, (1), 1–16, (2022).